

Solvent Effects on Photoinduced Electron-Transfer Reactions

Taeko Niwa, Koichi Kikuchi,* Noriyuki Matsusita, Michiko Hayashi, Tomoharu Katagiri, Yasutake Takahashi, and Tsutomu Miyashi

Department of Chemistry, Faculty of Science, Tohoku University,
Aoba, Aramaki, Aoba-ku, Sendai 980, Japan

Received: July 20, 1993*

Dependence of the fluorescence-quenching rate constant k_q , effective quenching distance r_q , and free radical yield Φ_R on the free enthalpy change ΔG_f of full electron transfer has been studied in dichloromethane by using anthracenecarbonitriles as electron-accepting fluorophores and amino- and methoxybenzenes as electron-donating quenchers. On the basis of the present data in dichloromethane and the previous data in acetonitrile, the solvent effects on the electron-transfer fluorescence-quenching mechanism and on the back electron-transfer reaction within the geminate radical ion pairs are elucidated.

1. Introduction

In previous work,^{1–5} we investigated the detailed mechanism of electron-transfer (ET) fluorescence quenching in a highly polar solvent, acetonitrile ($\epsilon = 37.5$ at 293 K⁶), by using several kinds of electron donor and acceptor (EDA) systems. It has been revealed that the quenching mechanism depends on the effective quenching distance r_q and the free enthalpy change ΔG_f of full ET⁷ in addition to the solvent polarity:

$$\Delta G_f = E_{1/2}^{\text{ox}} - E_{1/2}^{\text{red}} - e^2/\epsilon r_q - E(S_1) \quad (1)$$

Here $E_{1/2}^{\text{ox}}$, $E_{1/2}^{\text{red}}$, $E(S_1)$, and $-e^2/\epsilon r_q$ are the oxidation potential of electron donor, the reduction potential of electron acceptor, the excitation energy of fluorescent state, and the Coulomb attraction energy for oppositely monocharged radical ion pairs (RIP). In acetonitrile the switch over of the quenching mechanism occurs at around $\Delta G_f = -0.45$ eV. The quenching is due to an exciplex formation of the primary quenching products in the region, $\Delta G_f > -0.45$ eV, but a long-distance ET (i.e., ET not at contact distance) in the region, $\Delta G_f < -0.45$ eV. In the region $\Delta G_f = -0.45 \sim -2.0$ eV the primary quenching product is the ground-state geminate RIP, but in the region $\Delta G_f < -2.0$ eV it is the excited-state geminate RIP, the counterpart of which is electronically excited. In the region $\Delta G_f = -0.45 \sim -2.0$ eV it has been established that the rate k_b of back ET within the ground-state geminate RIP shows a bell-shaped dependence with respect to the free enthalpy change ΔG_b of back ET within the ground-state geminate RIP, in accordance with the Marcus theory⁸ for a long-distance ET:

$$\Delta G_b = E_{1/2}^{\text{red}} - E_{1/2}^{\text{ox}} + e^2/\epsilon r_q \quad (2)$$

In the present work we study the ET fluorescence quenching in a less polar solvent, dichloromethane (CH_2Cl_2 , $\epsilon = 8.93$ at 293 K⁶). The establishment of the quenching mechanism in CH_2Cl_2 is important particularly in the field of organic photochemistry, because a lot of studies on the photosensitized reactions have been performed in this solvent. The results are compared with the previous results⁵ in acetonitrile to establish the solvent effects on the ET fluorescence-quenching mechanism and also on the long-distance back ET reaction within the geminate radical ion pairs.

According to the Marcus theory,⁸ the solvent reorganization energy λ_s is given by eq 3:

$$\lambda_s = \frac{e^2}{2} \left(\frac{1}{r_a} + \frac{1}{r_d} - \frac{2}{r} \right) \left(\frac{1}{n^2} - \frac{1}{\epsilon} \right) \quad (3)$$

Here, r_a and r_d are the radii of the electron acceptor and donor, respectively, and r is the distance between the electron donor and acceptor. The refractive indexes n at 293 K are 1.34 and 1.42 for acetonitrile and CH_2Cl_2 , respectively.⁶ The dielectric constants ϵ at 293 K are 37.5 and 9.08 for acetonitrile and CH_2Cl_2 , respectively.⁶ Therefore, if the values for r_a , r_d , and r are not so different between the EDA systems employed in acetonitrile and in CH_2Cl_2 , the λ_s in CH_2Cl_2 is expected to be smaller than that in acetonitrile.

2. Experimental Section

The methods for synthesis and purification of 9-cyanoanthracene (CA), 9,10-dicyanoanthracene (DCA), 2,9,10-tricyanoanthracene (TrCA), and 2,6,9,10-tetracyanoanthracene (TeCA) have been reported elsewhere.⁹ Aniline (AN; Tokyo Kasei) and anisole (Tokyo Kasei) were purified by distillation under vacuum. 4-Cyanoaniline (CAN; Aldrich), anisidine (AS; Aldrich), and 1,4-phenylenediamine (PD; Nakarai) were sublimated under vacuum. *N,N,N',N'*-Tetramethyl-1,4-phenylenediamine (TMPD; Aldrich) was recrystallized from ethanol and sublimated under vacuum. 1,2-Dimethoxybenzene (1,2-DMB; Aldrich), 1,2,3-trimethoxybenzene (1,2,3-TMB; Aldrich), 1,2,4-trimethoxybenzene (1,2,4-TMB; Aldrich), and hexamethylbenzene (HMB; Aldrich) were used as received. Dichloromethane (CH_2Cl_2 ; SP grade, Nakarai) was dried with calcium hydride and distilled under argon atmosphere. Acetonitrile (SP grade, Kanto) was used as received.

Absorption spectra were recorded on a Hitachi 330 spectrophotometer. Fluorescence spectra and fluorescence excitation spectra were measured with a spectrophotometer built in this laboratory. The transient absorption spectra were measured by conventional flash photolysis. The free radical yield Φ_R and the triplet yield Φ_T in fluorescence quenching were determined by an emission-absorption flash photolysis method.^{9,10} The fluorescence lifetimes τ_f were measured by a Horiba NAES-550 time-correlated single photon counting fluorometer. The oxidation potential $E_{1/2}^{\text{ox}}$ and the reduction potential $E_{1/2}^{\text{red}}$ were measured in CH_2Cl_2 with 0.1 M tetra-*n*-butylammonium tetrafluoroborate as the supporting electrolyte and SCE as the reference electrode by using a Yanagimoto P-1000 polarography analyzer. The $E_{1/2}^{\text{red}}$ values for TrCA and TeCA were determined to be -0.79 and

* Author to whom correspondence should be addressed.

Abstract published in *Advance ACS Abstracts*, October 15, 1993.

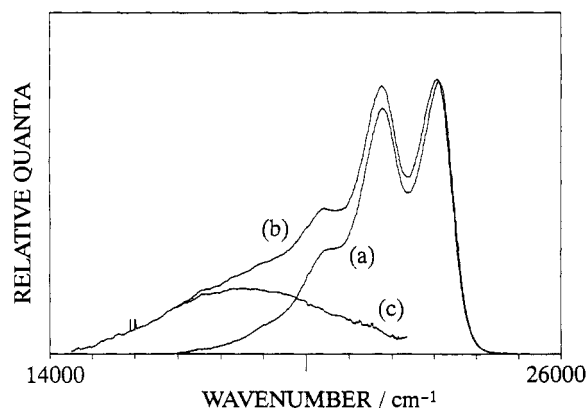


Figure 1. Fluorescence spectra of DCA in CH_2Cl_2 at the anisole concentrations of (a) 0 M and (b) 0.1 M and (c) their difference spectrum.

−0.37 V, respectively. The $E_{1/2}^{\text{red}}$ values for CA and DCA have been reported to be −1.70 and −0.89 V, respectively.¹¹ The $E_{1/2}^{\text{ox}}$ values for the quenchers have been determined as follows: 0.32 V for TMPD, 0.42 V for PD, 0.89 V for AS, 1.05 V for DPA, 1.07 V for AN, 1.44 V for CAN, 1.92 V for anisole, 1.74 V for 1,2-DMB, 1.58 V for 1,2,3-TMB, 1.28 V for 1,2,4-TMB, and 2.02 V for HMB.

Deaerated solutions were used to determine Φ_R and Φ_T . Aerated solutions were used to determine r_q and the fluorescence-quenching rate constant k_q . All measurements were made at 298 K.

3. Results and Discussion

The EDA complex formation in the ground state was checked by measuring the absorption spectra for all the sample solutions. A distinct EDA complex formation was observed for the systems TeCA–TMPD and TeCA–HMB. In the other systems, the EDA complex formation was not detected up to the quencher concentration 0.1–0.2 M. The equilibrium constants K_g for the systems TeCA–TMPD and TeCA–HMB were determined to be 0.75 and 1.5 M^{-1} at 298 K, respectively.

Figure 1 shows the fluorescence spectra of DCA in the absence (a) and the presence (b) of anisole (0.1 M). The spectra were normalized at the higher wavenumber region. The difference spectrum c between spectra a and b may be attributed to the exciplex fluorescence, because both spectral shape and location are characteristic for exciplex fluorescence.¹² Exciplex fluorescence was observed even for the following systems: CA–1,2,3-TMB, CA–1,2-DMB, and CA–HMB. It is noted that the fluorescence excitation spectrum at a higher quencher concentration (0.1–0.2 M) agrees with the absorption spectrum of free species even in the systems TeCA–TMPD and TeCA–HMB, indicating no emissivity of the EDA complex.

The fluorescence-quenching rate constants k_q have been determined from the Stern–Volmer plots for either the fluorescence intensity or the lifetime of free species at the lower quencher concentration, where the plots are linear. The effective quenching distance r_q may be determined by use of the modified Stern–Volmer equation derived by Weller:^{13,14}

$$\frac{I_f}{I_f^0} = \frac{\exp\{-V_D(I_f/I_f^0)^{1/2}[Q]\}}{1 + k_q\tau_f^0[Q]} \quad (4)$$

$$V_D = 4\pi N r_q^2 (D_a + D_d) \tau_f^0$$

$$k_q = 4\pi N r_q (D_a + D_d)$$

Here, I_f is the fluorescence intensity of free species. D_d and D_a are the diffusion coefficients for the electron donor and acceptor, respectively. Superscript “0” stands for the solution containing

TABLE I: Free Enthalpy Changes of Photoinduced ET in CH_2Cl_2 (ΔG_f), Fluorescence Quenching Rate Constants (k_q), and Effective Quenching Distances (r_q)

fluorescer	quencher	ΔG_f , eV	k_q , $10^{10} \text{ M}^{-1} \text{ s}^{-1}$	r_q , Å
CA	HMB	+0.32 ^a	—	—
CA	anisole	+0.22 ^a	0.002	—
CA	1,2-DMB	−0.04 ^a	0.20	—
CA	1,2,3-TMB	−0.13 ^a	0.17	—
CA	CAN	−0.27	0.31	4.3
CA	1,2,4-TMB	−0.43	1.2	4.3
DCA	anisole	−0.46	1.9	—
DCA	1,2-DMB	−0.55	1.5	5.6
CA	DPA	−0.58	1.6	5.4
CA	AS	−0.65	1.6	7.6
TeCA	HMB	−0.73	2.0	6.4
DCA	CAN	−0.81	1.4	6.5
DCA	1,2,4-TMB	−0.91	1.8	8.3
CA	PD	−1.10	2.2	8.5
DCA	DPA	−1.12	2.3	9.7
TeCA	1,2,3-TMB	−1.12	1.6	7.9
DCA	AN	−1.13	2.4	8.0
TeCA	CAN	−1.21	2.5	11
DCA	AS	−1.27	2.2	10
TeCA	1,2,4-TMB	−1.35	2.4	12
TeCA	DPA	−1.54	2.3	13
DCA	PD	−1.73	2.3	11
TeCA	AS	−1.74	2.5	12
DCA	TMPD	−1.81	2.3	12
TrCA	PD	−1.81	2.2	12
TrCA	TMPD	−1.91	2.2	12
TeCA	PD	−2.21	2.7	12
TeCA	TMPD	−2.31	2.0	11

^a Calculated by assuming $r_q = 4.3$ Å.

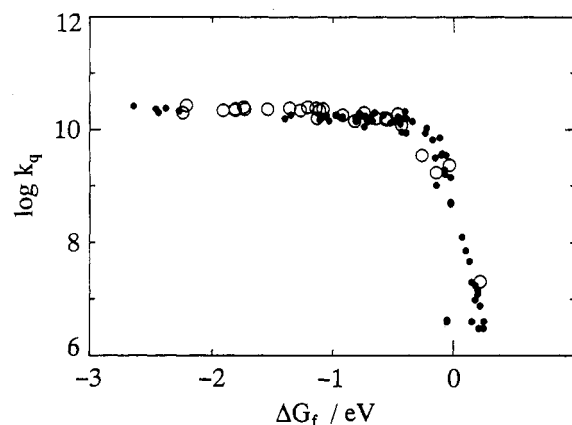


Figure 2. Plots of k_q versus ΔG_f : (O) in CH_2Cl_2 , (●) in acetonitrile.

no quencher. To determine r_q , we measured I_f at higher quencher concentrations such as 0.1–0.2 M. The fluorescence lifetimes τ_f^0 in CH_2Cl_2 were determined as follows: 14.5, 12.2, 14.8, and 14.4 ns in the deaerated solution and 12.5,¹¹ 12.2,¹¹ 14.2, and 13.0 ns in the aerated solution for CA, DCA, TrCA, and TeCA, respectively.

The values for k_q , r_q , and ΔG_f in CH_2Cl_2 are summarized in Table I. In CH_2Cl_2 , the Coulomb attraction energy $-e^2/\epsilon r_q$ cannot be neglected in the evaluation of ΔG_f , and it strongly depends on r_q . Therefore, we used the r_q 's listed in Table I to evaluate the ΔG_f 's in CH_2Cl_2 . The r_q 's for the EDA systems with $\Delta G_f > -0.2$ eV were assumed to be 4.3 Å. The $E(S_1)$'s in CH_2Cl_2 were determined to be 3.03, 2.89, 2.89, and 2.87 eV for CA, DCA, TrCA, and TeCA, respectively.

In Figure 2 we find that the ΔG_f dependence of k_q in CH_2Cl_2 agrees with that in acetonitrile, i.e., the Rehm–Weller (RW) relationship.⁷

In the region $\Delta G_f \geq -0.43$ eV, the r_q 's are close to the interplanar separation in the exciplex and charge-transfer complex. Exciplex fluorescence was observed for the systems CA–HMB, CA–1,2-DMB, DCA–anisole, and CA–1,2,3-TMB but not for the systems

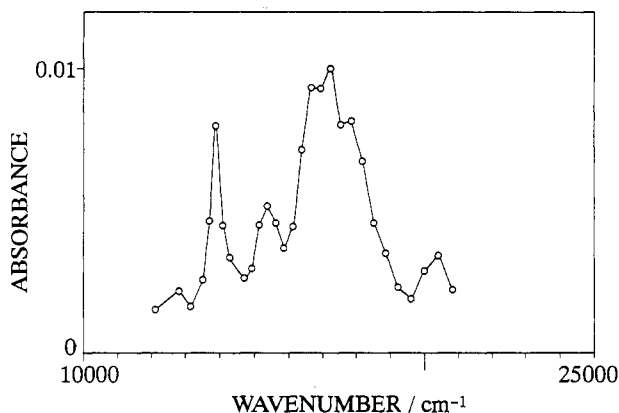


Figure 3. Transient absorption spectrum obtained for the deaerated CH₂Cl₂ solution containing 50 μ M TeCA and 6.3 mM PD (delay time, 100 μ s).

TABLE II: Free Radical Yields in CH₂Cl₂ (Φ_R), Triplet Yields (Φ_T), Free Enthalpy Changes of Back ET within the Ground-State Geminate RIP (ΔG_b), Rate Constants of Spin-Allowed Back ET within the Ground-State Geminate RIP (k_b), and Rate Constants of Geminate Radical Separation into Free Radicals (k_{esc})

fluorescer	quencher	Φ_R	Φ_T	$-\Delta G_b$, eV	$k_b, 10^{10} \text{ s}^{-1}$	$k_{esc}, 10^7 \text{ s}^{-1}$
TeCA	HMB	0.0041	0.002	2.14	0.099	0.41
DCA	CAN	0.0054	0.0038	2.07	0.083	0.45
DCA	1,2,4-TMB	0.0020	0.0016	1.97	0.87	1.7
DCA	AN	0.0014	0.0018	1.75	1.1	1.5
TeCA	1,2,3-TMB	0.0014	—	1.75	0.98	1.4
TeCA	CAN	0.0019	—	1.66	2.5	4.7
TeCA	1,2,4-TMB	0.0017	—	1.52	3.4	5.8
DCA	PD	0.0008	—	1.14	5.9	4.7
TeCA	AS	0.0020	—	1.13	2.9	5.9
TeCA	PD	0.0055	—	0.66	1.06	5.9
TeCA	TMPD	0.015	—	0.54	0.31	4.7

CA-anisole, CA-CAN, and CA-1,2,4-TMB. The intensity of exciplex fluorescence depends on the lifetime of the exciplex. Even if the exciplex fluorescence is not observed, it may be concluded that the fluorescence quenching is induced by the exciplex formation in the region $\Delta G_f \geq -0.46$ eV. In the region $\Delta G_f \leq -0.55$ eV the r_q 's are greater than 5 Å, and hence the quenching is induced by a long-distance ET.

Consequently, the switch over of the quenching mechanism occurs at around $\Delta G_f = -0.50$ eV in CH₂Cl₂. This switch-over ΔG_f is very close to that in acetonitrile, -0.45 eV.¹⁻⁵ This is reasonable, because the exciplex may be produced by the mixing of the locally excited (LE) state and the contact RIP state when the energy gap between these states is small.

Flashing of the CH₂Cl₂ solution containing both fluorescer and quencher gives the transition absorption due to the fluorescer radical anion and the quencher radical cation. In the case of the systems DCA-AN, DCA-1,2,4-TMB, DCA-CAN, and TeCA-HMB, the T-T absorption of fluorescer was observed in addition to the absorption of radical anion and radical cation. Figure 3 shows the transient absorption spectrum obtained for the deaerated solution containing 50 μ M TeCA and 6.3 mM PD. The absorption below 18 000 cm⁻¹ is ascribed to the TeCA radical anion TeCA^{-•}, and the broad band at around 20 000 cm⁻¹ is ascribed to the PD radical cation.

The free radical yields Φ_R and the triplet yields Φ_T in fluorescence quenching were determined as listed in Table II. We find that Φ_R decreases with a decrease in ΔG_f , passes through a minimum at -1.73 eV, and then increases.

If the fluorescence quenching is induced by a long-distance ET for producing the ground-state geminate RIP, the free radical

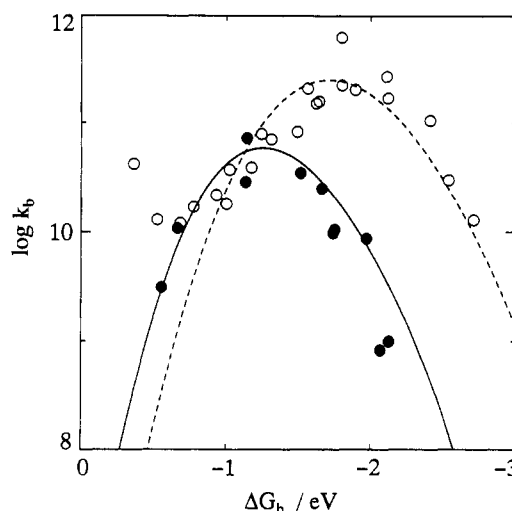


Figure 4. Plots of k_b versus ΔG_b : (●) in CH₂Cl₂, (○) in acetonitrile. Theoretical curves were depicted by eq 16 with the following fitting parameters: (—) $\lambda_v = 0.3$ eV, $h\nu = 1500$ cm⁻¹, $V = 18$ cm⁻¹, and $\lambda_S = 1.00$ eV; (---) $\lambda_v = 0.3$ eV, $h\nu = 1500$ cm⁻¹, $V = 39$ cm⁻¹, and $\lambda_S = 1.45$ eV.

yield Φ_R may be given by eq 5:

$$\Phi_R = k_{esc} / (k_{esc} + k_b) \quad (5)$$

When the energy $E(T_1)$ of the lowest triplet state of fluorescer is less than the energy $|\Delta G_b|$ of the ground-state geminate RIP, the fluorescer triplet may be produced by the spin-forbidden back ET within the ground-state geminate RIP. Then Φ_R and Φ_T are given by eqs 6 and 7:

$$\Phi_R = k_{esc} / (k_{esc} + k_b + k_{isc}) \quad (6)$$

$$\Phi_T = k_{isc} / (k_{esc} + k_b + k_{isc}) \quad (7)$$

Here, k_{esc} is the rate constant for the geminate RIP separation into the free radical ions and k_b and k_{isc} are the rate constants for the spin-allowed and the spin-forbidden back ET within the ground-state geminate RIP.

Only a few values for k_{esc} have been determined in acetonitrile: 5×10^8 s⁻¹ for the pyrene (Py)-*N,N*-dimethylaniline system,¹⁵⁻¹⁷ 0.8×10^9 s⁻¹ for perylene (Per)-tetracyanoethylene (TCNE), 1.7×10^9 s⁻¹ for 9,10-diphenylanthracene (DPA)-TCNE, 1.9×10^9 s⁻¹ for 1,12-benzoperylene (BPer)-TCNE, and 2.5×10^9 s⁻¹ for Py-TCNE.¹⁸ However, the k_{esc} in CH₂Cl₂ has not been determined yet. To determine the k_{esc} in CH₂Cl₂, therefore, we used the Tachiya method for the partially diffusion-controlled recombination of a pair of particles.¹⁹

According to the Tachiya method, the escape probability $\phi(r_0)$ for a pair of particles at the initial separation r_0 can be determined by using the following equations:

$$D \left[\nabla_{r_0}^2 \phi_0 - \frac{1}{kT} \nabla_{r_0} v(r_0) \cdot \nabla_{r_0} \phi_0 \right] = 0 \quad (8)$$

$$D \left[\frac{\partial \phi_0}{\partial r_0} \right]_{r_0=R} = p \phi_0(R) \quad (9)$$

$$\lim_{r_0 \rightarrow \infty} \phi_0(r_0) = 1 \quad (10)$$

Here, $v(r_0)$ is the interaction potential for two particles with initial separation r_0 , p is a recombination parameter with the dimension of cm s⁻¹, and D is the sum of the diffusion coefficients of two particles. R is the encounter separation. In the case of the back

TABLE III: Free Enthalpy Changes of Photoinduced ET in Acetonitrile (ΔG_f), Fluorescence-Quenching Rate Constants (k_q), Effective Quenching Distances (r_q), Free Radical Yields (Φ_R), Triplet Yields (Φ_T), Free Enthalpy Changes of Back ET within the Ground-State Geminate RIP (ΔG_b), and Rate Constants of Spin-Allowed Back ET within the Ground-State Geminate RIP (k_b)

fluorescer	quencher	$-\Delta G_f$, eV	k_q , $10^{10} \text{ M}^{-1} \text{ s}^{-1}$	r_q , Å	Φ_R	Φ_T	$-\Delta G_b$, eV	k_b , 10^{10} s^{-1}
CA	CAN	0.33	1.2	3.8	0.12	0.07	2.71	1.3
DCA	anisole	0.35	1.4	3.5	0.055	0.023	2.54	3.0
CA	AN	0.63	2.0	5.6	0.021	0.005	2.41	10.5
DCA	CAN	0.77	1.9	7.0	0.012	0.009	2.12	16.9
CA	AS	0.93	2.3	7.9	0.007	0.003	2.11	26.9
TrCA	CAN	1.00	2.0	9.3	0.008	—	1.89	20.5
DCA	AN	1.09	2.5	8.0	0.003	0.002	1.80	62.7
CA	PD	1.24	2.6	8.7	0.0078	—	1.80	22.3
TeCA	CAN	1.25	2.1	11	0.0085	—	1.64	16.0
DCA	DMA	1.27	2.7	10	0.010	<0.003	1.62	15.1
TrCA	AN	1.33	2.8	10	0.0072	—	1.56	21.1
CA	TMPD	1.40	3.0	—	0.020	—	—	—
DCA	AS	1.40	2.5	11	0.016	—	1.49	8.4
TeCA	AN	1.58	2.9	10	0.021	—	1.31	7.1
TrCA	AS	1.65	2.8	11	0.017	—	1.24	7.9
DCA	PD	1.72	2.8	11	0.034	—	1.17	3.9
TeCA	AS	1.89	2.6	14	0.054	—	1.00	1.8
DCA	TMPD	1.87	3.0	13	0.029	—	1.02	3.7
TrCA	PD	1.96	2.6	14	0.044	—	0.93	2.2
TrCA	TMPD	2.12	2.9	13	0.060	—	0.77	1.7
TeCA	PD	2.21	2.4	14	0.075	—	0.68	1.2
TeCA	TMPD	2.37	2.3	12	0.086	—	0.52	1.3
TeCA	BPB	2.53	2.3	8.2	0.042	—	0.36	4.2

ET within the oppositely monocharged geminate RIP, we have

$$v(r_0) = -e^2/\epsilon r_0 \quad (11)$$

From eqs 8–11 we obtain

$$\phi(R) = \frac{\{(Dr_c)/(pR^2)\} \exp(-r_c/R)}{\{(Dr_c)/(pR^2) - 1\} \exp(-r_c/R) + 1} \quad (12)$$

Here r_c is the Onsager distance:

$$r_c = e^2/\epsilon kT \quad (13)$$

Φ_R is defined as $\phi(R)$ at $R = r_q$. Therefore, we obtain from eq 12

$$\Phi_R = \frac{Dr_c}{r_q^3 \{\exp(r_c/r_q) - 1\}} \bigg/ \left[\frac{Dr_q}{r_q^3 \{\exp(r_c/r_q) - 1\}} + \frac{p}{r_q} \right] \quad (14)$$

As p/r_q corresponds to k_b , we have

$$k_{\text{esc}} = \frac{Dr_c}{r_q^3 \{\exp(r_c/r_q) - 1\}} \quad (15)$$

Equation 15 indicates that k_{esc} depends on r_q . The validity of eq 15 can be confirmed as follows: In the case of the photoinduced ET between aromatic molecules in acetonitrile at 298 K, we can assume $D = 3.5 \times 10^{-5} \text{ cm}^2 \text{ s}^{-1}$.^{13,14} The r_q 's have been determined to be 7.9 Å for the system Per-TCNE, 8.7 Å for the system DPA-TCNE, and 11 Å for the systems Py-TCNE and BPer-TCNE.²⁰ Then the k_{esc} 's are calculated to be $1.9 \times 10^9 \text{ s}^{-1}$ for Per-TCNE, $1.8 \times 10^9 \text{ s}^{-1}$ for DPA-TCNE, $1.4 \times 10^9 \text{ s}^{-1}$ for Py-TCNE, and BPer-TCNE. They agree with the values of k_{esc} for these EDA systems reported by Mataga et al.¹⁸

The sum D of the diffusion coefficients of two particles is expressed as $D = kT/6\pi\eta$.¹² The viscosity coefficient η is 1.2 times greater in CH_2Cl_2 than in acetonitrile: 0.325 cP at 303 K and 0.375 cP at 288 K for acetonitrile and 0.393 cP at 303 K and 0.449 cP at 288 K for CH_2Cl_2 .⁶ In the calculation of k_{esc} in CH_2Cl_2 , therefore, we used $D = 2.9 \times 10^{-5} \text{ cm}^2 \text{ s}^{-1}$. The k_{esc} 's have been calculated according to eq 15, using the r_q 's listed in Table I. Then, the k_b 's can be calculated from the Φ_R 's and the Φ_T 's by use of eq 3 or eqs 4 and 5. The values for Φ_R , Φ_T , ΔG_b , k_b , and k_{esc} are summarized in Table II. In Figure 4, the k_b 's are plotted with respect to ΔG_b (closed circles).

When the back ET within the geminate RIP takes place at a fixed distance of the pair, the rate of back ET may be given by eq 16:^{21–23}

$$k_b = \frac{\pi}{\hbar^2 \lambda_S k_B T} |V|^2 \sum_{w=0}^{\infty} \left(\frac{e^{-S} S^w}{w!} \right) \exp \left\{ -\frac{(\lambda_S + \Delta G_b + w\hbar\nu)^2}{4\lambda_S k_B T} \right\} \quad (16)$$

where $S = \lambda_S/\hbar\nu$.

As seen in Table I, the r_q 's in CH_2Cl_2 are nearly constant in the region $\Delta G_f < -1.2 \text{ eV}$ or $\Delta G_b > -1.7 \text{ eV}$. The back ET may begin to take place at r_q , which is the initial separation of the geminate RIP. Therefore, the plot of k_b versus ΔG_b in CH_2Cl_2 may be fitted with eq 16 in the region $\Delta G_b > -1.7 \text{ eV}$. The plot is well reproduced by eq 16 as shown in Figure 4 (full line), when the following fitting parameters are adopted: $\lambda_S = 1.00 \text{ eV}$, the reactant vibrational reorganization energy $\lambda_r = 0.3 \text{ eV}$, the electron coupling matrix element $V = 18 \text{ cm}^{-1}$, and the average energy of active vibrational mode $\hbar\nu = 1500 \text{ cm}^{-1}$.

The values for ΔG_f , k_q , r_q , Φ_R , Φ_T , ΔG_b , and k_b in acetonitrile⁵ are summarized in Table III, where some new data are included. All the values were determined in the same manner as those in CH_2Cl_2 .

The k_b 's in acetonitrile are also plotted in Figure 4 (open circles). In the case of the systems TrCA-TMPD, TeCA-PD, and TeCA-BPB, the quenching is induced by a long-distance ET for producing the excited-state geminate RIP.⁵ Therefore, the plot may be fitted with eq 16 only in the region $-2.0 < \Delta G_f < -1.25 \text{ eV}$ or $-1.6 < \Delta G_b < -0.9 \text{ eV}$, where r_q is assumed to be constant, $12 \pm 2 \text{ Å}$. The plot is well reproduced by eq 16 in a wide region of ΔG_b as shown in Figure 4 (broken line), when the following fitting parameters are adopted: $\lambda_S = 1.45 \text{ eV}$, $\lambda_r = 0.3 \text{ eV}$, $V = 39 \text{ cm}^{-1}$, and $\hbar\nu = 1500 \text{ cm}^{-1}$. It is noted that both the solvent reorganization energy λ_S and the electron coupling matrix element V decrease with a decrease in the solvent polarity and that the k_b in CH_2Cl_2 is greater than that in acetonitrile in the region $\Delta G_b > -1.0 \text{ eV}$.

Figure 5 shows that the ΔG_f dependence of r_q in acetonitrile is the same as that in CH_2Cl_2 . In the region $\Delta G_f > -1.2 \text{ eV}$, the r_q increases with a decrease in ΔG_f in agreement with eq 3: λ_S increases with an increase in r_q , and hence the ET occurring at a greater r_q becomes favored in the more negative region of

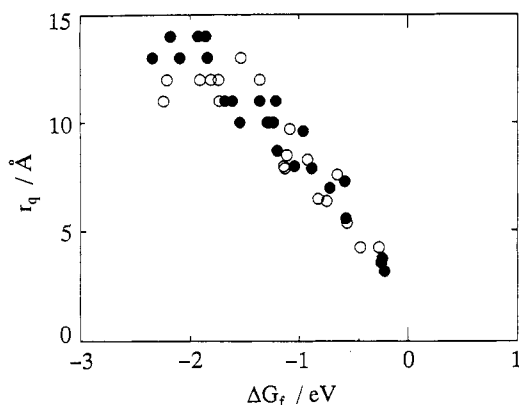


Figure 5. Plots of r_q versus ΔG_f : (O) in CH_2Cl_2 , (●) in acetonitrile.

ΔG_f , although V decreases with increase in r_q .²⁴ In the region $\Delta G_f = -1.2 \sim -2.4$ eV, the r_q is supposed to be 12 ± 2 Å.

According to eq 3, λ_S depends on n and ϵ in addition to r_a , r_d , and r . If r_a , r_d , and r are the same in CH_2Cl_2 and acetonitrile, we obtain the ratio

$$\frac{\lambda_S(\text{CH}_3\text{CN})}{\lambda_S(\text{CH}_2\text{Cl}_2)} = \frac{1/n^2(\text{CH}_3\text{CN}) - 1/\epsilon(\text{CH}_3\text{CN})}{1/n^2(\text{CH}_2\text{Cl}_2) - 1/\epsilon(\text{CH}_2\text{Cl}_2)} = 1.37$$

Both r_a and r_d are nearly constant in a series of the EDA systems. The fitting parameters for the plots of k_b versus ΔG_b in both CH_2Cl_2 and acetonitrile were determined for the geminate RIP with the separation $r_q = 12 \pm 2$ Å. Therefore, the ratio obtained from the ΔG_b dependence of k_b in CH_2Cl_2 and acetonitrile, $\lambda_S(\text{CH}_3\text{CN})/\lambda_S(\text{CH}_2\text{Cl}_2) = 1.45/1.00 = 1.45$, can be compared with the above ratio. The agreement between the theory and the experiment is very good.

The EDA systems in CH_2Cl_2 are the same as those in acetonitrile. Nevertheless, the value for V is 2.4 times greater in acetonitrile than in CH_2Cl_2 . It is suggested, therefore, that the electronic interaction between the electron donor and acceptor is enhanced with an increase in the solvent polarity. Then no difference in the ΔG_f dependence of k_q between CH_2Cl_2 and acetonitrile may qualitatively be attributed to the difference in λ_S , because λ_S depends on the refractive index and the dielectric constant but not on the type of ET reaction.²⁵ The decrease in λ_S from 1.45 to 1.00 eV may give rise to an increase in k_q in the region $\Delta G_f = -0.5 \sim -1.0$ eV, where the quenching is induced by a long-distance ET. Such a phenomenon for k_b is clearly demonstrated in Figure 4.

It is noted that in the region $\Delta G_b > -1.0$ eV k_b deviates upward from the theoretical curve with increasing ΔG_b in acetonitrile but not in CH_2Cl_2 . In this region, i.e., in the systems TeCA-TMPD and TeCA-PD, the generation of the excited-state geminate RIP as the primary quenching product is energetically possible both in acetonitrile and CH_2Cl_2 , because the excitation energy $E(\text{TeCA}^+ \cdot)$ for TeCA⁺ is determined to be 1.72 eV from the absorption maximum located at $13\,900\text{ cm}^{-1}$ in Figure 2. The free enthalpy change $\Delta G_b^* (= \Delta G_b - E(\text{TeCA}^+ \cdot))$ for back ET within the excited-state geminate RIP in CH_2Cl_2 is calculated to be -2.26 and -2.38 eV for the systems TeCA-TMPD and TeCA-PD, respectively. Thus, the rate constants k_b^* for back ET within the excited-state geminate RIP in CH_2Cl_2 are estimated by using these ΔG_b^* values and eq 16 with the fitting parameters in CH_2Cl_2 : $k_b^* = 1.4 \times 10^9\text{ s}^{-1}$ for the TeCA-TMPD system and $7.2 \times 10^8\text{ s}^{-1}$ for the TeCA-PD systems. In CH_2Cl_2 , therefore, the k_b^* 's are not greater than the corresponding k_b 's. Then, almost all the excited-state geminate RIP may deactivate into the ground-state geminate RIP, and hence the k_b determined from eq 5 and Φ_R does not deviate from the theoretical curve.

4. Summary

The ΔG_f dependence of k_q is the same in acetonitrile and CH_2Cl_2 : k_q increases with a decrease in ΔG_f in the region $\Delta G_f > -0.5$ eV, and it is close to the diffusion-controlled limit in the region $\Delta G_f < -0.5$ eV. As illustrated in Figure 4, this is the result of two contrary effects of V and λ_S on k_q . The ΔG_f in CH_2Cl_2 strongly depends on r_q . If the k_q is in the downhill region of the RW relationship, therefore, the r_q in CH_2Cl_2 may be determined by fitting the k_q with the RW relationship. The ΔG_f dependence of r_q is the same in acetonitrile and CH_2Cl_2 : r_q increases with a decrease in ΔG_f in the region $\Delta G_f > -1.2$ eV and is 12 ± 2 Å in the region $-2.4 < \Delta G_f < -1.2$ eV. The switch-over $\Delta G_f = -0.50$ eV of the quenching mechanism in CH_2Cl_2 is very close to that in acetonitrile, -0.45 eV. The ΔG_f value of $-0.45 \sim -0.50$ eV is considered to be a critical value for producing an exciplex by the mixing between the LE state and the contact RIP state. The solvent dependence of $\lambda_S (= 1.00$ eV in CH_2Cl_2 and 1.45 eV in acetonitrile) is well predicted by the Marcus theory, eq 3. According to the Tachiya method for the partially diffusion-controlled recombination of a pair of particles, the k_{esc} strongly depends on r_q in a less polar solvent. The k_{esc} 's in CH_2Cl_2 are 2 orders of magnitude or more smaller than those in acetonitrile. This is the principal reason why the Φ_R 's in CH_2Cl_2 are about 1 order of magnitude lower than those in acetonitrile.

Acknowledgment. The authors are greatly indebted to Dr. M. Tachiya (National Institute of Materials and Chemical Research) for his helpful comments for evaluating the k_{esc} 's in dichloromethane and to Prof. H. Kokubun for his generous support.

References and Notes

- (1) Kikuchi, K.; Niwa, T.; Takahashi, Y.; Ikeda, H.; Miyashi, T.; Hoshi, M. *Chem. Phys. Lett.* **1990**, *173*, 421–424.
- (2) Kikuchi, K.; Takahashi, Y.; Katagiri, T.; Niwa, T.; Hoshi, M.; Miyashi, T. *Chem. Phys. Lett.* **1991**, *180*, 403–408.
- (3) Kikuchi, K.; Hoshi, M.; Niwa, T.; Takahashi, Y.; Miyashi, T. *J. Phys. Chem.* **1991**, *95*, 38–42.
- (4) Kikuchi, K.; Takahashi, Y.; Hoshi, M.; Niwa, T.; Katagiri, T.; Miyashi, T. *J. Phys. Chem.* **1991**, *95*, 2378–2381.
- (5) Kikuchi, K.; Katagiri, T.; Niwa, T.; Takahashi, Y.; Suzuki, T.; Ikeda, H.; Miyashi, T. *Chem. Phys. Lett.* **1992**, *193*, 155–160.
- (6) Riddick, J. A.; Bunger, W. B. *Organic Solvents*; in *Techniques of Chemistry*; Weissberger, A., Ed. Wiley: New York, 1970; Vol. II.
- (7) Rehm, D.; Weller, A. *Isr. J. Chem.* **1970**, *8*, 259–271.
- (8) Marcus, R. A. *J. Phys. Chem.* **1956**, *24*, 966–978; *Annu. Rev. Phys. Chem.* **1964**, *15*, 155–196.
- (9) Kikuchi, K.; Takahashi, Y.; Koike, K.; Wakamatsu, K.; Ikeda, H.; Miyashi, T. *Z. Physik. Chem. (Munich)* **1990**, *167*, 27–39.
- (10) Kikuchi, K.; Kokubun, H.; Koizumi, M. *Bull. Chem. Soc. Jpn.* **1968**, *41*, 1545–1551.
- (11) Karatsu, T.; Kobayashi, H.; Shinkai, E.; Kitamura, A. *Chem. Lett.* **1992**, 2131–2134.
- (12) Birks, J. B. *Photophysics of Aromatic Molecules*; Wiley: London, 1970.
- (13) Leonhardt, H.; Weller, A. *Ber. Bunsen-Ges. Phys. Chem.* **1963**, *67*, 791–795.
- (14) Knibbe, H.; Rehm, D.; Weller, A. *Ber. Bunsen-Ges. Phys. Chem.* **1968**, *72*, 257–263.
- (15) Weller, A. *Z. Physik. Chem. (Munich)* **1982**, *130*, 129–138.
- (16) Schulten, K.; Stark, H.; Weller, A.; Werner, H. J.; Nickel, B. *Z. Physik. Chem. (Munich)* **1976**, *101*, 371–390.
- (17) Wener, H. J.; Stark, H.; Weller, A. *J. Chem. Phys.* **1978**, *68*, 2419–2426.
- (18) Mataga, N.; Asahi, T.; Kanda, Y.; Okada, T. *Chem. Phys.* **1988**, *127*, 249–261.
- (19) Sano, H.; Tachiya, M. *J. Chem. Phys.* **1979**, *71*, 1276–1282.
- (20) Kikuchi, K.; Niwa, T.; Takahashi, Y.; Ikeda, H.; Miyashi, T. *J. Phys. Chem.* **1993**, *97*, 5070–5073.
- (21) Ulstrup, J.; Jortner, J. *J. Chem. Phys.* **1975**, *63*, 4358–4368.
- (22) Siders, P.; Marcus, R. A. *J. Am. Chem. Soc.* **1981**, *103*, 741–747.
- (23) Miller, J. R.; Beitz, J. V.; Huddleston, R. K. *J. Am. Chem. Soc.* **1984**, *106*, 5057–5068.
- (24) Tachiya, M.; Murata, S. *J. Phys. Chem.* **1992**, *96*, 8441–8444.
- (25) Tachiya, M. *Chem. Phys. Lett.* **1989**, *159*, 505–510.